



## Article

# Transcriptomic Database Analysis of Magnesium Transporter (MGT) Gene Family in Pear (*Pyrus bretschneideri*) Revealed Its Role in Reproductive Stage Development

Yuchen Ma <sup>1,†</sup>, Baopeng Ding <sup>2,3,†</sup>, Khushboo Khan <sup>4</sup>, Yujing Lin <sup>1</sup>, Ahmad Ali <sup>5,\*</sup> and Liulin Li <sup>1,\*</sup>

<sup>1</sup> College of Horticulture, Shanxi Agricultural University, Taigu, Jinzhong 030801, China; mayc0429@163.com (Y.M.); linyujing0206@163.com (Y.L.)

<sup>2</sup> Engineering Research Center of Coal-Based Ecological Carbon Sequestration Technology of the Ministry of Education, Shanxi Datong University, Datong 037049, China; dingbaopeng2006@163.com

<sup>3</sup> Key Laboratory of Graphene Forestry Application of National Forest and Grass Administration, Shanxi Datong University, Datong 037049, China

<sup>4</sup> Faculty of Crop Production Sciences, The University of Agriculture Peshawar, Peshawar 25120, Khyber Pakhtunkhwa, Pakistan; yousafkh1020@gmail.com

<sup>5</sup> National Engineering Research Center for Sugarcane, Fujian Agriculture and Forestry University, Fuzhou 350002, China

\* Correspondence: ahmad03348454473@yahoo.com (A.A.); tgliulin@163.com (L.L.)

† These authors contributed equally to this work.

**Abstract:** The membrane proteins of the magnesium transporter (MGT) family are essential to Mg homeostasis. However, there has not been a comprehensive study of MGT in pear. The 17 MGT that were renamed to *PbMGT1–17* in this study were found in the pear genome database. Phylogenetically, *PbMGT* proteins were categorized into three groups, namely NIPA, MRS2, and CorA. The majority of *PbMGT* were hydrophobic proteins situated on the chloroplast, according to the characterization study. Members of the same group shared comparable conserved motifs and gene structure, as revealed by motif and exon/intron analysis. The application of gene ontology (GO) and *cis*-elements has demonstrated that *PbMGT* genes exhibit a high degree of sensitivity to stressors and take part in chloroplast development and Mg<sup>+</sup> ion transport. It was discovered by tissue-specific expression analysis that *PbMGT* genes might have a role in the development of organs. The critical significance of *PbMGT* was shown through comprehensive expression in five pear cultivars at various fruit developmental stages. The *PbMGT5* gene was significantly expressed throughout fruit development, suggesting a role in the setting and ripening processes of pear fruits. For the first time, our research brought attention to the function of *PbMGT* genes as they relate to fruit development. Our research is likely to serve as an incentive for the development of pear breeding initiatives in the future.

**Keywords:** MGT; pear; fruit development; bioinformatics; gene family



**Citation:** Ma, Y.; Ding, B.; Khan, K.; Lin, Y.; Ali, A.; Li, L. Transcriptomic Database Analysis of Magnesium Transporter (MGT) Gene Family in Pear (*Pyrus bretschneideri*) Revealed Its Role in Reproductive Stage Development. *Horticulturae* **2024**, *10*, 333. <https://doi.org/10.3390/horticulturae10040333>

Academic Editor: Aisheng Xiong

Received: 1 March 2024

Revised: 19 March 2024

Accepted: 27 March 2024

Published: 28 March 2024



**Copyright:** © 2024 by the authors. Licensee MDPI, Basel, Switzerland. This article is an open access article distributed under the terms and conditions of the Creative Commons Attribution (CC BY) license (<https://creativecommons.org/licenses/by/4.0/>).

## 1. Introduction

Magnesium (Mg) is an essential mineral for all living cells because it plays a role in numerous critical cellular processes [1]. For example, over 300 enzymes, including kinase, polymerase, and H<sup>+</sup> ATPase, rely on magnesium as a cofactor to function [2]. Furthermore, being the essential component of chlorophyll, magnesium influences both the pace of photosynthesis and the growth of plants [3]. Mg absorption, translocation, and cell storage are all facilitated by magnesium transporter (MGTs) genes found in plants [3,4]. Three categories of MGT proteins, including mitochondrial RNA splicing 2 (MRS2) magnesium-binding domain, magnesium/cobalt transporter (CorA), and non-imprinted in Prader–Willi/Angelman syndrome (NIPA), have been identified based on their sequence structures [5]. MGT proteins were investigated in the model plant *Arabidopsis* [5]. The CorA protein, one of the MGTs, was initially discovered in plants and

bacteria, specifically in *Salmonella typhimurium* [6]. A tripeptide conserved sequence called glycine–methionine–asparagine (GMN) and two or three transmembrane (TM) domains at their C-terminal ends identify the MRS2 and CorA proteins [6]. Although NIPAs' architectures include many TM, our understanding of the NIPA class is limited [7]. The *MGT* gene family has been identified and researched in a variety of plants, including *Arabidopsis*, *Triticum turgidum*, *Camelina sativa*, *Pyrus communis*, and others, because of the significant function that magnesium plays in plants [7]. In addition, various plant species carried out experimental characterization of the function of recognized *MGT* genes.

To regulate magnesium levels, *MGT* genes are found in many plant tissues, such as roots, flowers, leaves, and stems [7–10]. Research has shown that certain root-specific *MGTs*, such as *OsMGT1* in *Oryza sativa* and *AtMGT6* in *Arabidopsis thaliana*, are involved in magnesium uptake from the soil [11]. The *AtMGT9* is a Mg transporter that moves Mg from root to shoot tissues [12]. In addition, *AtMGT5* and *AtMGT9* have a role in the formation of pollen in *Arabidopsis* [12]. A subset of *MGT* proteins is involved in intracellular magnesium distribution and accumulation; these proteins are found in the membranes of many cellular organelles [6]. As an example, in *Arabidopsis*, at least three of the magnesium transporters (*AtMGT2*, *AtMGT3*, and *AtMGT10*) are responsible for vacuolar magnesium accumulation and chloroplast magnesium homeostasis, respectively [12]. Some studies have shown that *MGTs* can make plants more resistant to harmful conditions. The *OsMGT1* gene was found to assist in rice's tolerance to salt stress. Furthermore, there is evidence that the expression of *MGT* genes positively correlates with plants' ability to tolerate aluminum (Al) stress [13]. It appears that elevating *MGT* activity and enhancing Mg uptake are crucial to mitigate the harmful effects of certain ions and elements.

Among the many temperate Rosaceae fruit species, the pear stands out as an economically significant tree [14,15]. The first recorded use of it dates back over 30,000 years ago; therefore, its history of cultivation is extensive [14]. Among the many species of pears found in the genus *Pyrus* are the following: *Pyrus communis*, *Pyrus bretschneideri*, *Pyrus ussuriensis*, *Pyrus pyrifolia*, and *Pyrus sinkiangensis*. The genomes of three highly representative pear species—the Chinese white pear ('Dangshansuli'), the European pear ('Bartlett'), and a wild pear species (*Pyrus betuleafolia*, 'Shanxi Duli')—have been made public [16,17]. Genome sequencing in pears lays the groundwork for future molecular biology and pear genomics research.

Through this study, we deduced the expression patterns and evolutionary expansion of the *MGT* superfamily genes present in these pear genomes. Afterward, we conducted a screening to identify the *MGT* members that are necessary for pear development. Bioinformatic, qRT-PCR, and transcriptome analysis uncovered the candidate gene's potential functional involvement in pear reproductive biology.

## 2. Material and Methods

### 2.1. RNA Sequencing of 5 Pear Cultivars

A total of 35 samples' (five species X seven stages) RNA was extracted from fruit flesh. An Illumina standard mRNA-Seq Prep Kit (TruSeq RNA and DNA Sample Preparation Kits version 2) was used for construction of RNA sequencing libraries. Single-end RNA-seq data were generated with a length of 49 bp. Reads were filtered and trimmed, and then they were mapped onto "Dangshansuli" (*Pyrus bretschneideri*) CDS sequences using SOAPaligner software [18].

### 2.2. Identification of Isolation of *MGT* Genes from the Pear Genome

The BLAST algorithm in Ensembl Plants was used to query the genomes of pear against the *MGT* proteins of *Arabidopsis* to discover all sequences related to the *MGT* family. To ensure that *MGT* domains were present, the nonredundant sequences of *MGTs* were examined using the CDD search and the Pfam database following the method of [19]. The instability index (GRAVY), isoelectric points (pI), and molecular weight (MW) of *MGTs* were predicted using the ProtParam tool. This study used Plant-mPLOC ([http:](http://)

[//www.csbio.sjtu.edu.cn/bioinf/plant-multi/#](http://www.csbio.sjtu.edu.cn/bioinf/plant-multi/#), accessed on 10 February 2024) as a tool to determine the subcellular localization of all *PbMGT* genes and their proteins.

### 2.3. Physical Location and Synteny of MGT Genes

Extracting gff3-files from the *P. bretschneideri* genome database and mapping them to chromosomes using TBtools (Toolbox for biologists) (v0.6655) determined the *PbMGT* genes' chromosomal distribution [20]. The following criteria were used to define gene duplication: (1) the alignment length was required to encompass more than 90% of the longer gene; (2) the aligned region had to have an identity more significant than 90%; and (3) for closely related genes, only one duplication event was considered.

### 2.4. Phylogenetic Analysis of MGT Proteins

The *Arabidopsis* and pear MGT amino acid sequences were utilized to construct a phylogenetic tree. The initial stage was aligning all sequences using Clustal-Omega, a multiple alignment program [21,22]. After that, the results of the Clustal-Omega were sent to the IQ-TREE website <http://iqtree.cibiv.univie.ac.at> (accessed on 10 February 2024) to estimate the phylogenetic relationships of MGTs by employing the maximum likelihood (ML) approach with a total of 1000 bootstrap replicates. Finally, the iTOL version 5 tool was used to create the phylogenetic tree of MGT proteins [23].

### 2.5. Gene Structure and Conserved Motif Analysis

The *P. bretschneideri* sequencing database was queried for details regarding the *PbMGT* gene family, such as accession number, chromosomal location, ORF length, and exon–intron structure. The Gene Structure Display Server (<http://gsds.cbi.pku.edu.cn/>, accessed on 12 February 2024) generated each gene's exon, intron, and UTR (untranslated region) distribution patterns by comparing the *P. bretschneideri* genome with CDS. Using the following parameters, the MEME tool (<http://meme-suite.org/index.html>, accessed on 14 February 2024) was used to examine the *PbMGT* protein motif. Each sequence must only include one motif instance, with a maximum of one occurrence per site. Ten motifs were to be discovered, and their breadth may be anywhere from six to one hundred. The software TBtools (Toolbox for Biologists) (v0.6655) was used to visualize these motifs [20].

### 2.6. Interactive Protein Partners

To build the network of protein–protein interactions between pear MGTs, the sequences of all MGTs were uploaded to the STRING v11.5 database <https://cn.string-db.org/>, accessed on 14 February 2024. The maximum number of interactors was set to 5 for the first shell, and for the second shell, it was set to 10. Lastly, Cytoscape v3.8.2 (<https://cytoscape.org/>, accessed on 10 February 2024) was used to depict the interaction networks.

### 2.7. Gene Ontology Analysis of *PbMGT* Genes

Additionally, *PbMGT* protein sequences were analyzed using the GO tool Blast2GO (Version 2.7.2) (<http://www.blast2go.com>) (accessed on 3 February 2024) [24]. By repeating the steps outlined in earlier research with [25], we were able to reassemble the three categories into which the cellular component GO categorization, molecular functions, and biological processes fell.

### 2.8. Promoter Analysis of *PbMGT* Genes

Each MGT gene's upstream region (1500 bp of ATG) in pear was screened using the PlantCARE [26] approach to identify the known cis-regulatory elements involved in growth, hormone response, and stress. The last step was to classify the cis-regulatory components based on their roles. The tool is referenced as [20].

### 2.9. Prediction of Targeted miRNAs

The genome sequences of 17 *PbMGT* genes were compared to miRNA sequences from the psRNA Target Server (<https://www.zhaolab.org/psRNATarget/>) (accessed on 2 February 2024) using the default parameters to predict miRNA [27]. Next, we followed the identical steps as our earlier work and ran the interaction through Cytoscape (<https://cytoscape.org/>) (accessed on 2 February 2024). Finally, we utilized Adobe Illustrator to improve visualization.

### 2.10. Prediction of 3D Protein Structures

The 3D configuration of the *PbMGT1* and *PbMGT2* proteins was acquired using the Phyre2 server, following the methodology outlined by [28]. The proteins underwent water molecule exclusion using Accelrys Discovery Studio v4.1 software and were subsequently visualized using pyMOL, following the methodology outlined by [29].

### 2.11. Microarray Expression Analysis of *PbMGT* Gene Family

The tissue-specific expression data was retrieved from our RNA-seq library. To investigate the expression patterns of the *PbMGT* gene family in *P. bretschneideri*, the researchers consulted five RNA-seq datasets released by [18], including *Pyrus bretschneideri* (*Pbr*), *Pyrus communis* (*Pco*), *Pyrus pyrifolia* (*Ppy*), *Pyrus sinkiangensis* (*Psi*), and *Pyrus ussuriensis* (*Pus*). Fruit-setting (15 DAB, period 1 [S1]), physiological fruit-dropping (30 DAB, period 2 [S2]), fruit rapid enlargement (55 DAB, period 3 [S3]), a month after fruit enlargement (85 DAB, period 4 [S4]), premature (115 DAB, period 5 [S5]), mature (varies by species, period 6 [S6]), and fruit senescence [S7] were collected in the transcriptomes. The parameters generated a heatmap using the log<sub>2</sub>(fold change) transformed values of each gene in the *PbMGT* family and the FPKM (fragments per kilobase of transcript per million fragments mapped) value for each gene. The distance measurement method used was Pearson correlation coefficient. The clustering method used was average linkage.

### 2.12. Statistical Analysis

The criterion for significantly differential expression was chosen at  $|\log_2(\text{fold change})| > 1.5$  and  $p\text{-value} < 0.005$ . Expression data were processed, grouped, and presented using TBtools (Toolbox for biologists) v0.6655 [20].

## 3. Results

An extensive search of the *Arabidopsis thaliana* (*AtMGT*) protein sequence was conducted to retrieve the *PbMGT* genes stored in the pear database. After repetitive and duplicated sequences were removed, 17 *PbMGT* genes were identified for additional experimental and bioinformatic study (Table 1). Measuring the deduced protein length using the Protpram service showed that *PbMGT* ranged in size from 175 bp (*PbMGT15*) to 497 bp (*PbMGT12*). *PbMGT1* had the highest molecular weight (55.14 kDa), while *PbMGT15* had a lower weight at 19.97 kDa. The isoelectric point (pI) values of the *PbMGT* protein sequence varied between 4.55 (*PbMGT6*) and 8.77 (*PbrMGT10*). According to subcellular localization, *PbMGT* genes were distributed in different organelles, such as the nucleus, chloroplast, and cell membrane.

**Table 1.** *PbMGT* gene family obtained from *P. bretschneideri* genome database.

Locus ID	Gene	Chr.	Start	End	No. AA	MW (kDa)	PI	SL
<i>Pbr035629.1</i>	<i>PbMGT1</i>	5	11530499	11533234	499	55.14	4.95	Nucleus
<i>Pbr025298.1</i>	<i>PbMGT2</i>	5	19052560	19055228	454	50.32	5.22	Nucleus
<i>Pbr026553.1</i>	<i>PbMGT3</i>	8	4019326	4022927	463	52.08	8.38	Chloroplast
<i>Pbr026552.1</i>	<i>PbMGT4</i>	8	4025306	4029889	465	51.96	5.77	Chloroplast
<i>Pbr009062.1</i>	<i>PbMGT5</i>	10	10014987	10017700	407	45.22	4.71	Nucleus
<i>Pbr018771.1</i>	<i>PbMGT6</i>	10	15755036	15756903	301	33.22	4.55	Nucleus

Table 1. Cont.

Locus ID	Gene	Chr.	Start	End	No. AA	MW (kDa)	PI	SL
<i>Pbr029967.3</i>	<i>PbMGT7</i>	13	4534375	4536674	432	48.69	5.35	Nucleus
<i>Pbr014721.1</i>	<i>PbMGT8</i>	13	5286444	5292607	397	44.21	4.85	Chloroplast
<i>Pbr018319.1</i>	<i>PbMGT9</i>	14	9847472	9851439	463	52.35	5.05	Nucleus
<i>Pbr003194.1</i>	<i>PbMGT10</i>	15	41303362	41306863	464	52.12	8.77	Chloroplast
<i>Pbr001806.1</i>	<i>PbMGT11</i>	16	9145142	9149449	422	Undefined	Undefined	Nucleus
<i>Pbr036745.1</i>	<i>PbMGT12</i>	Scaffold732.0	29832	38286	497	54.97	4.97	Nucleus
<i>Pbr039912.1</i>	<i>PbMGT13</i>	Scaffold868.0	54166	57561	478	53.48	7.31	Chloroplast
<i>Pbr039915.1</i>	<i>PbMGT14</i>	Scaffold868.0	96276	99671	478	53.48	7.31	Chloroplast
<i>Pbr040583.1</i>	<i>PbMGT15</i>	Scaffold899.0	81130	82089	175	19.97	4.99	Cell membrane
<i>Pbr040585.1</i>	<i>PbMGT16</i>	Scaffold899.0	100391	103310	478	53.70	8.03	Chloroplast
<i>Pbr040588.1</i>	<i>PbMGT17</i>	Scaffold899.0	140233	143150	464	52.06	7.32	Chloroplast

Chromosome: Chr, Amino Acid: AA, Molecular Weight: MW, Isoelectric Point: PI, Subcellular Location: SL.

### 3.1. Domain Organization of PbMGT Proteins

The Pfam and smart domain databases were used to identify the conserved domain of PbMGT proteins. Based on the obtained results, all the PbMGT proteins consist of the highly conserved Mrs2\_Mfm1p-like domain (Figure 1). The size of the domain ranges from 350 to 400 bp in length, covering almost the entire protein sequence of PbMGT proteins.

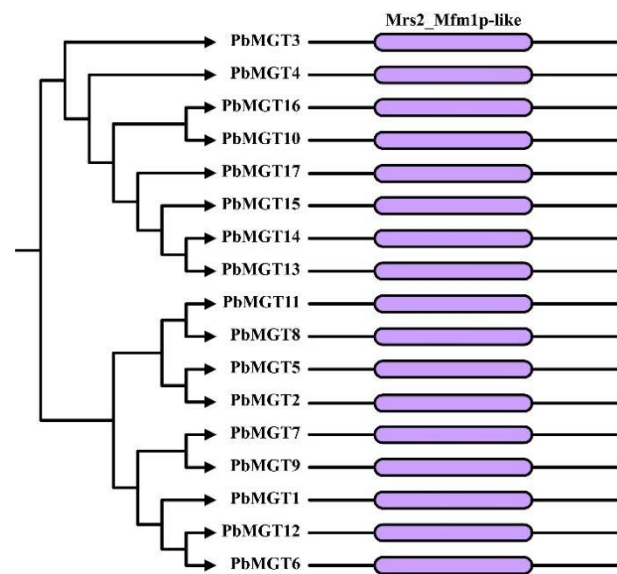
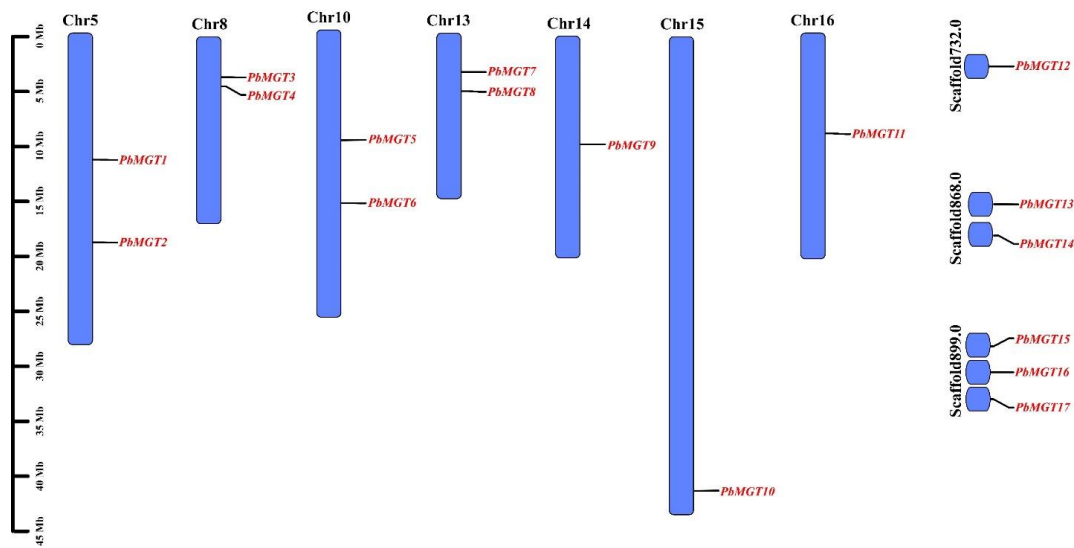


Figure 1. Schematic representation of conserved domain in PbMGT proteins.

### 3.2. Chromosomal Localization

The pear genome database was used to establish the chromosomal position of the *PbMGT* gene family, and then the figure was made with the help of Tbttools (Figure 2). The findings revealed that the pear's *PbMGT* genes were dispersed across its chromosomes. Chromosomes 14, 15, and 16 each accounted for a single gene. All the other chromosomes possessed a majority of two genes on their arms. Several *PbMGT* genes were positioned on scaffold chromosomes.



**Figure 2.** Physical mapping of *PbMGT* genes on the chromosomes of pear.

### 3.3. Phylogenetic Analysis

The phylogenetic analysis sheds light on the evolutionary composition of pear *MGT* genes by analyzing their protein sequences (Figure 3). Categorically, the *PbMGT* together with *AtMGT* genes are classified into three groups (MRS2, CorA, and NIPA), with MRS2 and NIPA having the largest number of genes (10 genes). The CorA group was recorded with the least number of genes, with six genes from pear and Arabidopsis.

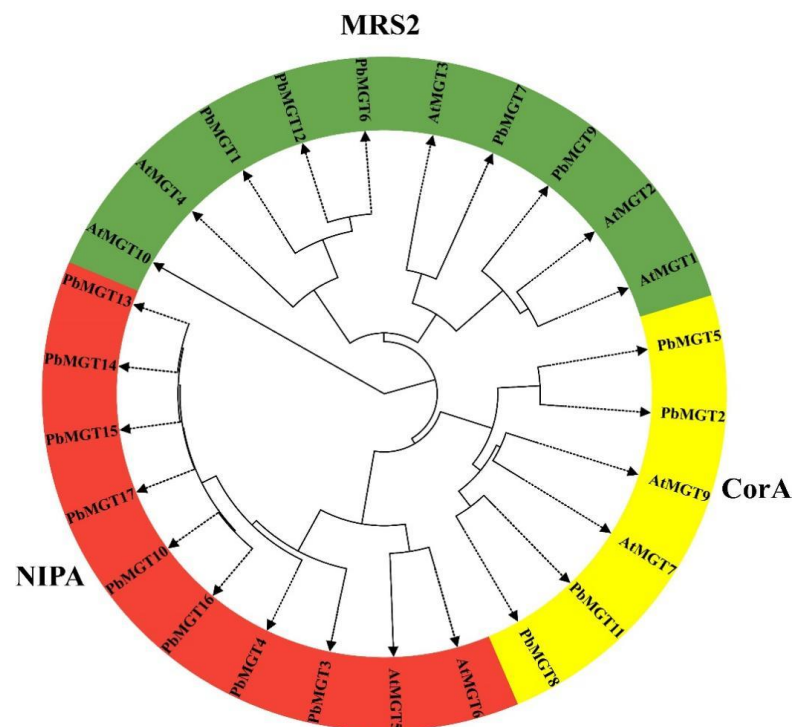


**Figure 3.** Phylogenetic analysis classified *MGT* proteins from different plant species into three subgroups based on complete protein sequences. All *MGT* proteins were highlighted in red (NIPA), yellow (CorA), and green (MRS2). Protein sequences of pear and *arabidopsis* were used to draw the phylogenetic tree using neighbor joining model.

### 3.4. Synteny Analysis of *PbMGT* Genes

Synteny links between the pear and *Arabidopsis* genomes were also examined to determine the likely roles of the *PbMGT* genes. In the *Arabidopsis* (~60%) and pear (~76%) genomes, all the *PbMGT* genes had synteny links, as shown in Figure 4. During genome evolution, the pear chromosomes' close evolutionary links and extensive rearrangement events can be demonstrated by these comprehensive synteny relations at the gene level.

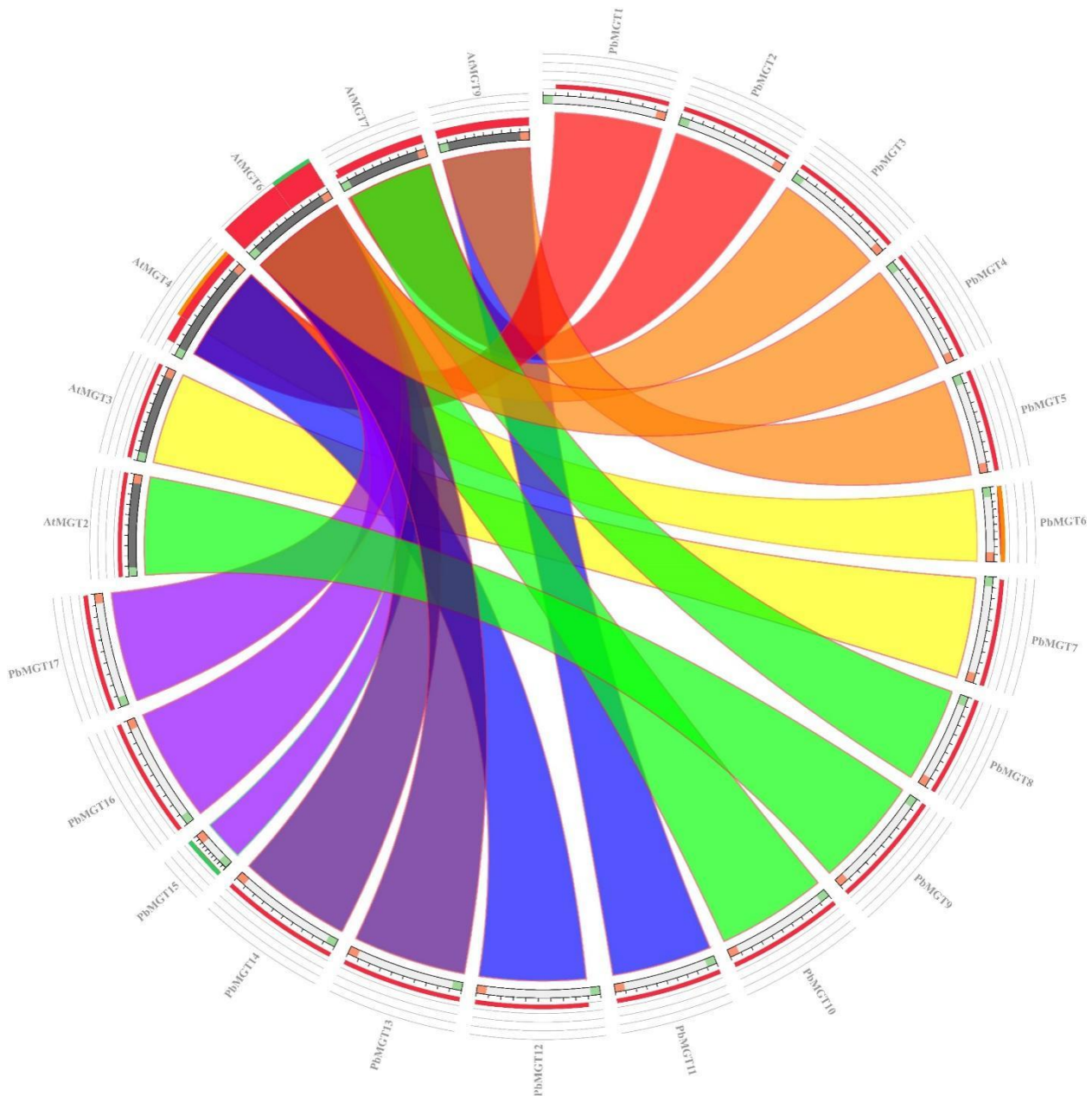


**Figure 4.** Syntenic analysis of pear MGT and *arabidopsis* MGT proteins. Rainbow grey scale parameters were set to draw the Circos plot. Purple ribbons indicate a collinear relationship among the blocks in the whole genome, and red ribbons show *PbMGT* paralogs. Green color ribbons represent segmentally duplicated genes.

### 3.5. Gene Structure and Conserved Motifs Analysis

To comprehend the structural elements of the *PbMGT* gene family, the whole CDS and genomic sequences were obtained from the pear genome database (Figure 5). The *PbMGT5* and *PbMGT2* contain the highest number of exons with a total of 11 exons. The majority of

*PbMGT* genes accounted for four exons, at least. Similarly, the highest number of *PbMGT5* and *PbMGT2* holds the highest number of introns on their genomic structure. The *PbMGT4*, *PbMGT8*, *PbMGT10*, and *PbMGT12* were the only genes with UTR (upstream/downstream) on their genomic region.

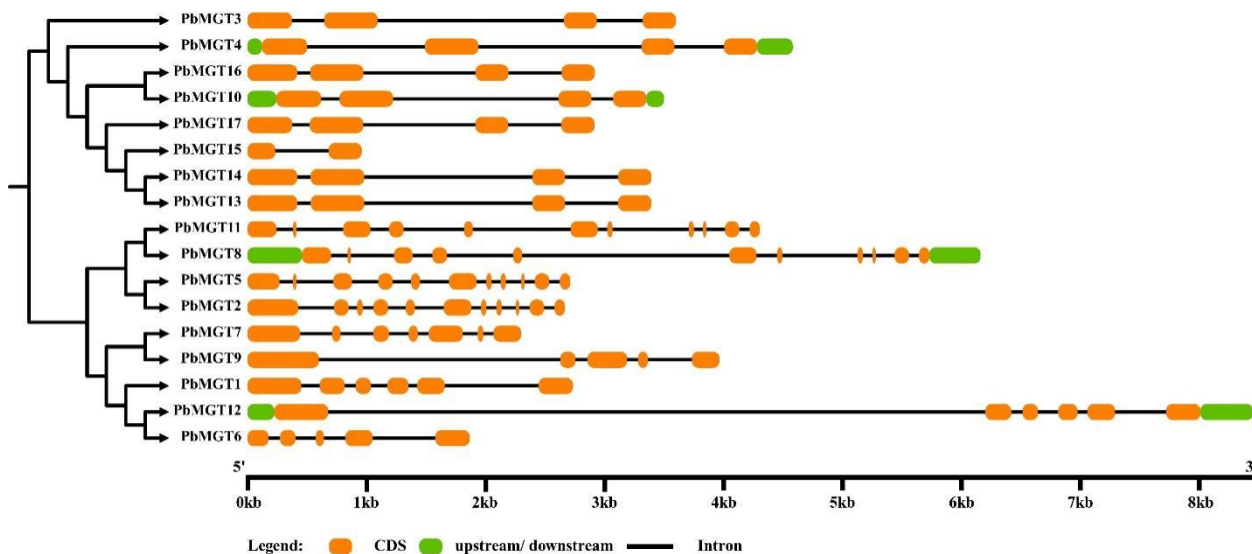


**Figure 5.** Locations and lengths of the exons and introns of *PbMGT* family genes are depicted with exons as filled orange sticks, introns as thin black lines, and UTRs as green bars at the ends. The gene structures were illustrated using the GSDS online database.

Ten conserved motifs in the amino acid sequence of *PbMGT* genes were discovered using MEME analysis ( $E$ -value  $> 1.2 \times 10^{-221}$ ) (Figure 6). Motif 9 was recorded in all the *PbMGT* proteins except *PbMGT6* and *PbMGT15*. Motif 10 was present in *PbMGT3*, *PbMGT4*, *PbMGT16*, *PbMGT10*, *PbMGT17*, *PbMGT14*, and *PbMGT13* but missed out in other *PbMGT* proteins. Motif 1 was recorded in all the *PbMGT* proteins.

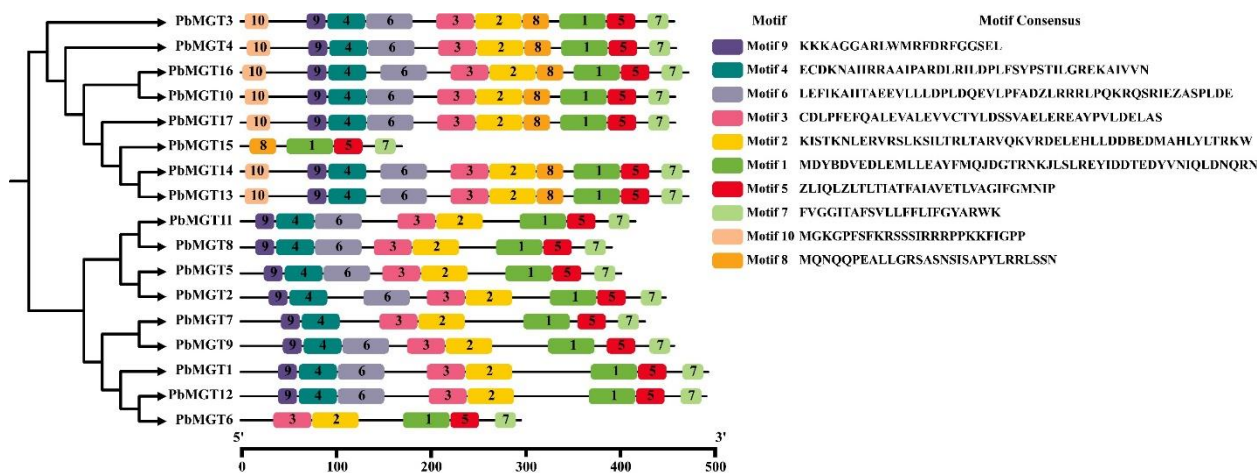


**Figure 6.** Conserved motif analysis of *PbMGT* indicates 10 predicted motifs identified by the MEME database online and visualized by Tbttools software V2.069.

### 3.6. Gene ontology Enrichment Analysis

To have a better grasp of the possible roles played by specific gene families before conducting wet lab experiments, gene ontology (GO) analysis is commonly employed. The protein sequences were used to analyze the GO enrichment terms of the *PbMGT* genes (Figure 7). As is obvious from the name, *PbMGT* genes are highly involved in Mg ion

transmembrane and transporter. The prominent biological processes, such as chlorophyll biosynthesis and leaf senescence, are the hallmarks of PbMGT proteins. Other key features of PbMGT proteins are stomata regulation and ATPase activity (Figure 7).

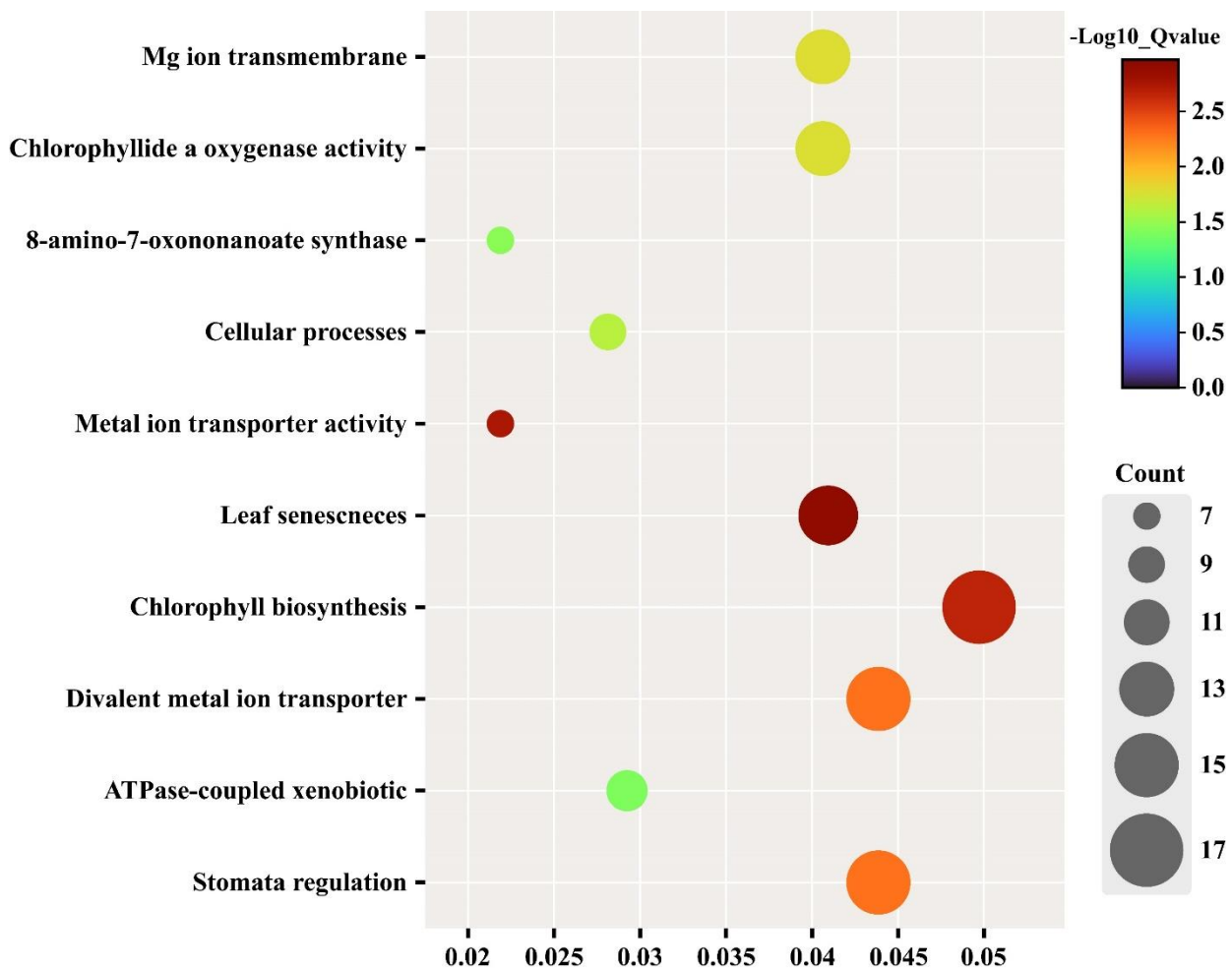


**Figure 7.** Gene ontology analysis of *PbMGT* genes shows the distribution of various biological, molecular, and cellular processes.

### 3.7. Protein–Protein Interaction

The protein interaction network drawn from the String online database provides ample clues regarding the posited interacted roles of PbMGT proteins (Figure 8). For instance, our reference protein PbMGT1 displayed strong interaction with LTP14 (Lipid transfer proteins14), and an array for MGT proteins. Other prominent interactive members include HIPP28. HIPP28 is from Arabidopsis plant protein with a heavy metal domain and isoprenylation motif. The MHX gene encodes an  $Mg^{2+}/H^{+}$  exchanger and also displays strong interaction with our reference protein (Figure 8).

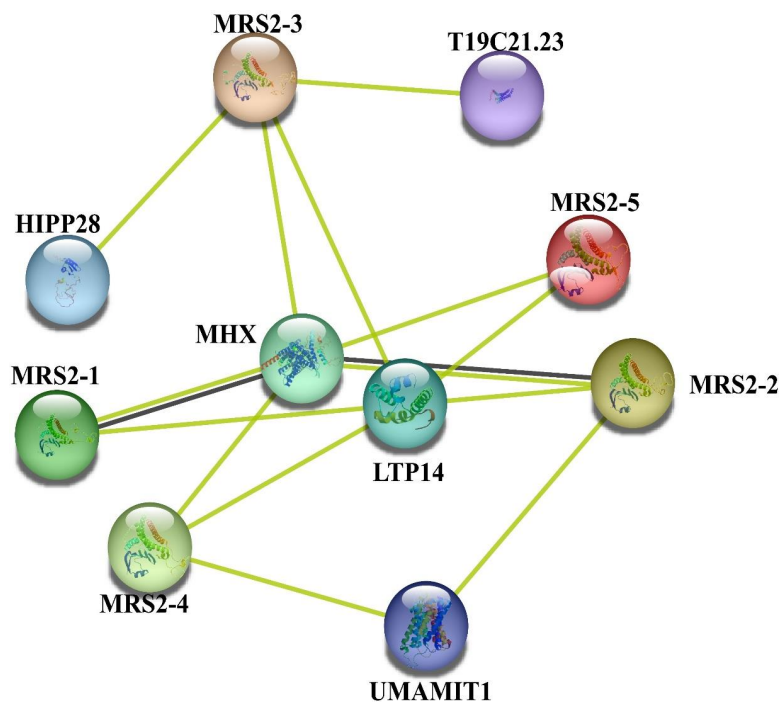


**Figure 8.** Interactive protein network of PbMGT. All the PbMGT proteins were used as reference which displayed interaction with numerous other key proteins.

### 3.8. D Protein Structure of PbMGT

With a confidence level of over 90%, the three-dimensional structures of the MGT protein were predicted, and their possible active sites were also shown. In all MGT, CorA-like, and NIPA proteins, the three-dimensional structures of MGT proteins showed a characteristic frame with many parallel  $\beta$ -turns and  $\alpha$ -helices. Here, we provided the 3D model of PbMGT1 and PbMGT2 to understand their structural characteristics (Figure 9). The findings suggest that these proteins have a common structural feature. The PbMGT1 and PbMGT2 proteins show a high degree of homology, particularly in their catalytic sites and areas that bind metal ions, despite some discernible sequence differences (Figure 9). protein structure analysis (ProSA) results showed that each protein model had sections with a significant rate of residues with the lowest energy, verifying the modeling quality in diverse parts of these proteins.

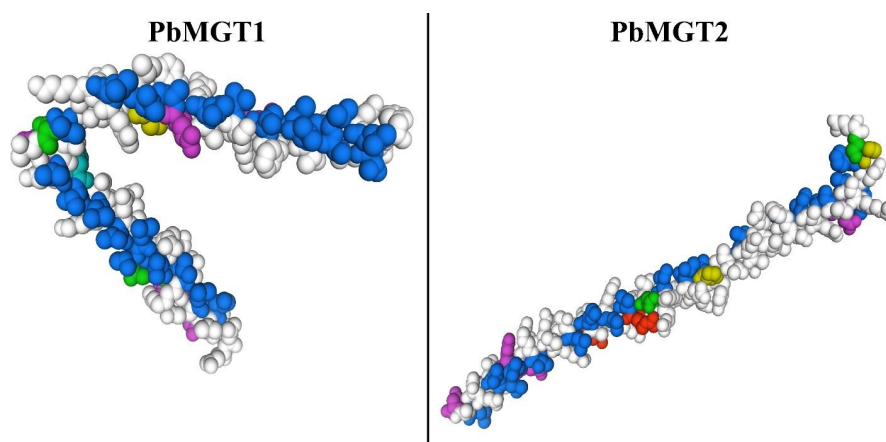


**Figure 9.** Three-dimensional protein homology of PbMGT1 and PbMGT2. The ExPasy server was used to draw the 3D protein structure. Protein–protein docking, and hydrogen bond interactions observed in the binding interface region of PbMGT1 and PbMGT2 by molecular docking technique.

### 3.9. Cis-Acting Elements of Promoter Region *PbMGT* Genes

The PLANTCARE online database was used to retrieve and analyze the 1.5 kb promoter region of *PbMGT* genes upstream of ATG (start codon) to understand transcriptional regulation. Many cis-elements associated with growth, stress, and hormonal control were detected (Figure 10). For example, the *PbMGT1* has the highest number of hormonal-responsive cis-elements followed by general stress-related elements. Other members of the *PbMGT* gene family displayed an almost similar pattern in terms of cis-elements distribution (Figure 10). The presence of MYB, ABRE, and drought-responsive cis terms in the upstream region can be coordinated with the stomatal regulation GO terms (Figure 7) of *PbMGT* genes.

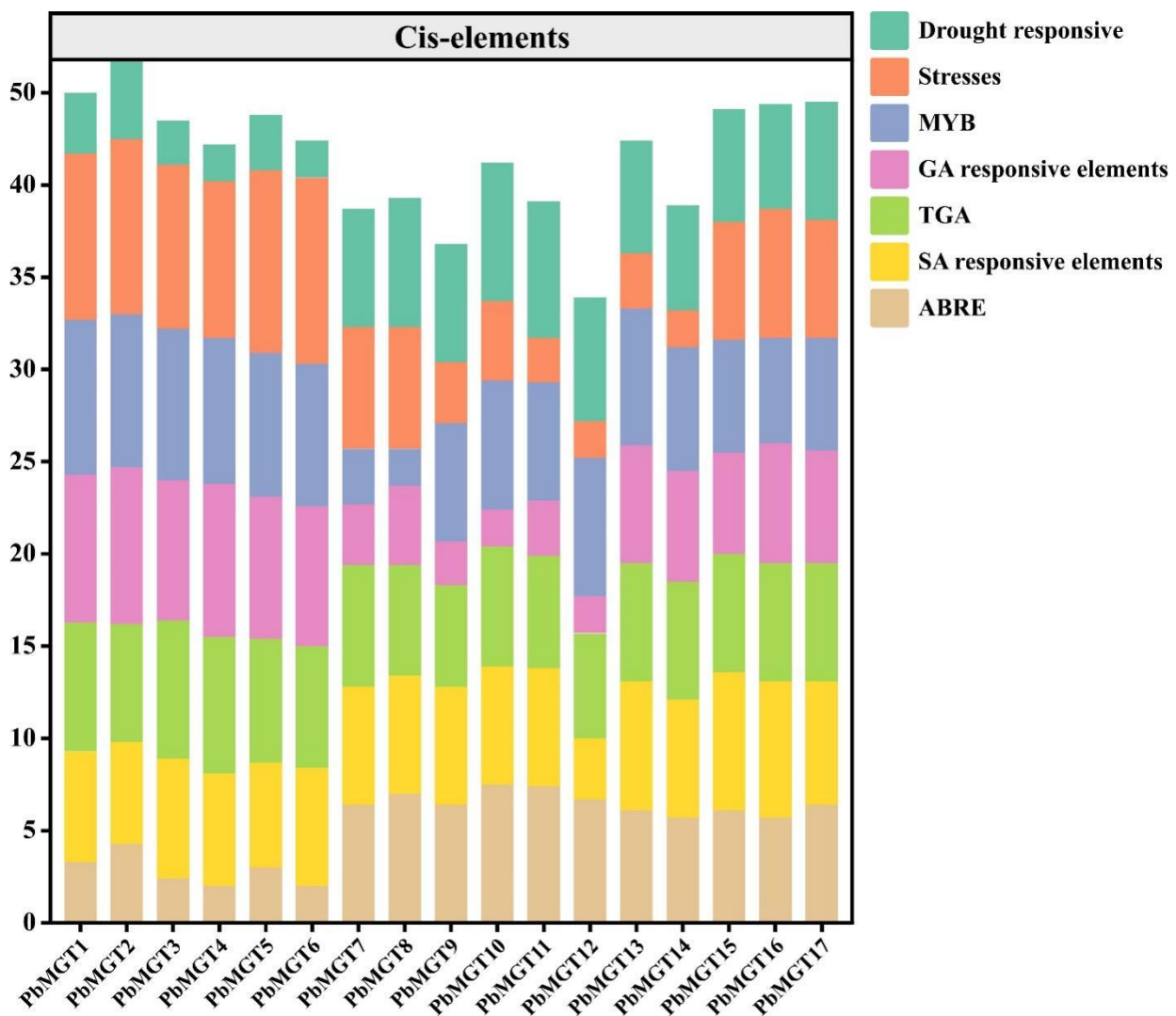


**Figure 10.** cis-acting elements presented in the 2KB upstream region of *PbMGT* genes. Various categories of cis-elements were retrieved, and the picture was drawn on GraphPad Prism.

### 3.10. Predicted Targeted miRNAs by *PbMGT* Genes

We blasted the downloaded sequences of all pear miRNAs against the CDS sequence of *PbMGT* genes to predict the target miRNAs cleaved to those genes. Our miRNA library includes several *PbMGT* genes, including *PbMGT7*, *PbMGT1*, *PbMGT3*, *PbMGT8*, and several others (Figure 11). Prominent miRNA families, such as miR164 and miR169, were cleaved to *PbMGT7*. Other critical miRNA families include miR156, miR172, miR173,

miR414, and miR854 (Figure 11). These miRNAs are, by and large, driving a significant number of biological processes in plants.

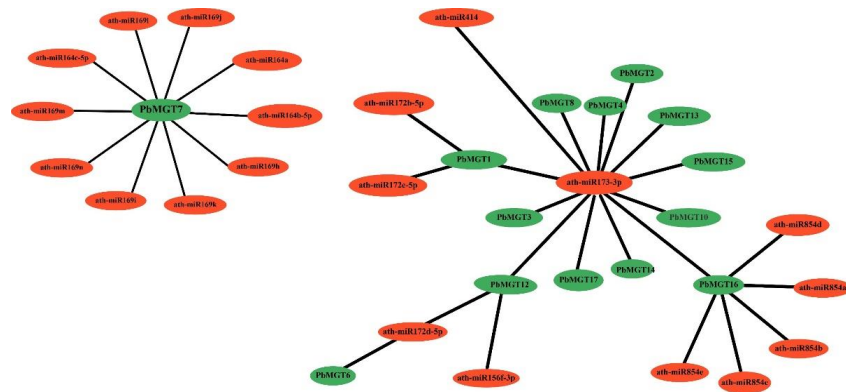


**Figure 11.** Predicted targeted miRNAs cleaved by *PbMGT* genes. Cytoscape was used to draw the miRNAs-gene network. The *PbMGT* genes are represented with green color, whereas the red circles represent targeted miRNAs.

3.11. Spatial Expression of *PbMGT* Genes

Using the RNA-seq data, we examined the expression of *PbMGT* genes in various organs of *P. bretschneideri* (Figure 12). The tissue that was used to assess the expression of *PbMGT* genes included stem, leaves, buds, fruit, ovary, and sepals and petals. Most *PbMGT* genes displayed lower expression patterns in all the vegetative tissues except the *PbMGT9*. The *PbMGT9* showed higher expression in the stem. In reproductive tissues, the *PbMGT3*, *PbMGT7*, *PbMGT9*, and *PbMGT10* have higher expression in all the designated reproductive tissues. Other *PbMGT* genes demonstrated lower expression in the reproductive tissues (Figure 12).

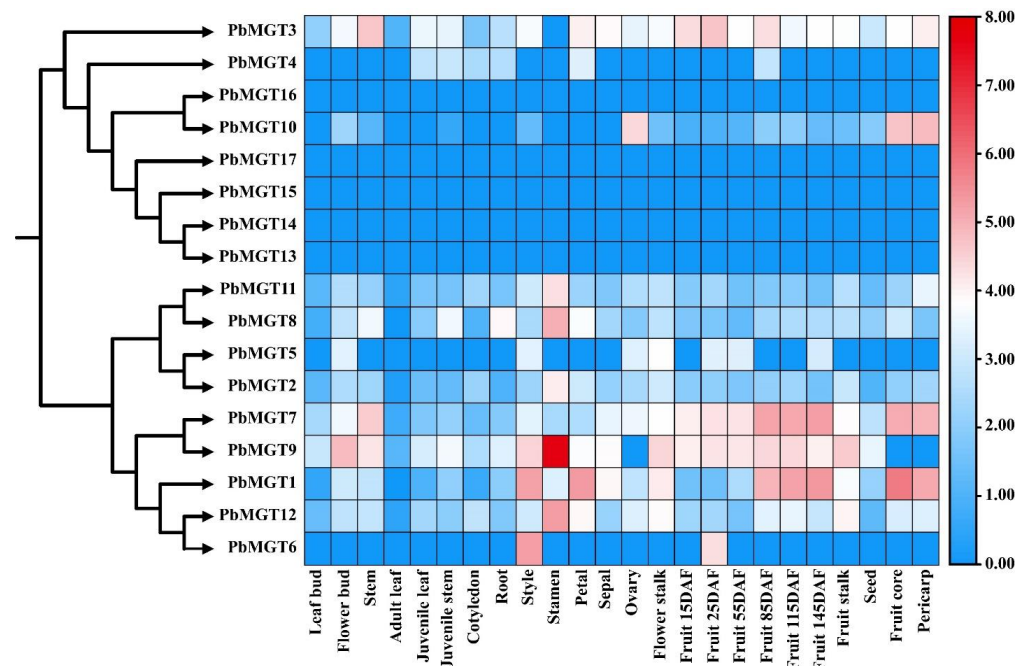


**Figure 12.** Heatmap of *PbMGT* gene family transcript expression profiles from *Pyrus bretschneideri* RNA-seq data. Each column's colored boxes show gene expression relative to log<sub>2</sub> (fold change). Data were obtained from the stem, fruits, ovary, leaf, bud, petal, and sepal. Levels of expression are displayed as red for higher and blue for lower. The Ttools program was used to create the heatmap.

### 3.12. Expression of *PbMGT* Gene Family in Five Pear Species

Five different pear cultivars were utilized in this study, including Pbr (*Pyrus bretschneideri*), Pco (*Pyrus communis*), Ppy (*Pyrus pyrifolia*), Psi (*Pyrus sinkiangensis*), and Pus (*Pyrus ussuriensis*). Further investigation on the expression of *PbMGT* genes was conducted. Samples were obtained at specific time points during the growth and development of the fruit. We found several genes highly expressed at various phases of fruit development. In all five pear cultivars tested, for instance, the *PbMGT1* had a high mRNA level at S1–S7 (Figure 13). At S1–S7, the *PbMGT4* and *PbMGT5* were substantially expressed, following a similar pattern. The majority of the *PbMGT* genes displayed constant expression trends in all five species, mirroring their conserved functional role (Figure 13). Among the five pear species (Pbr, Pco, Ppy, Psi, and Pus), the *PbMGT5* stood out for its consistently high expression pattern from S1 to S7 in fruit development.

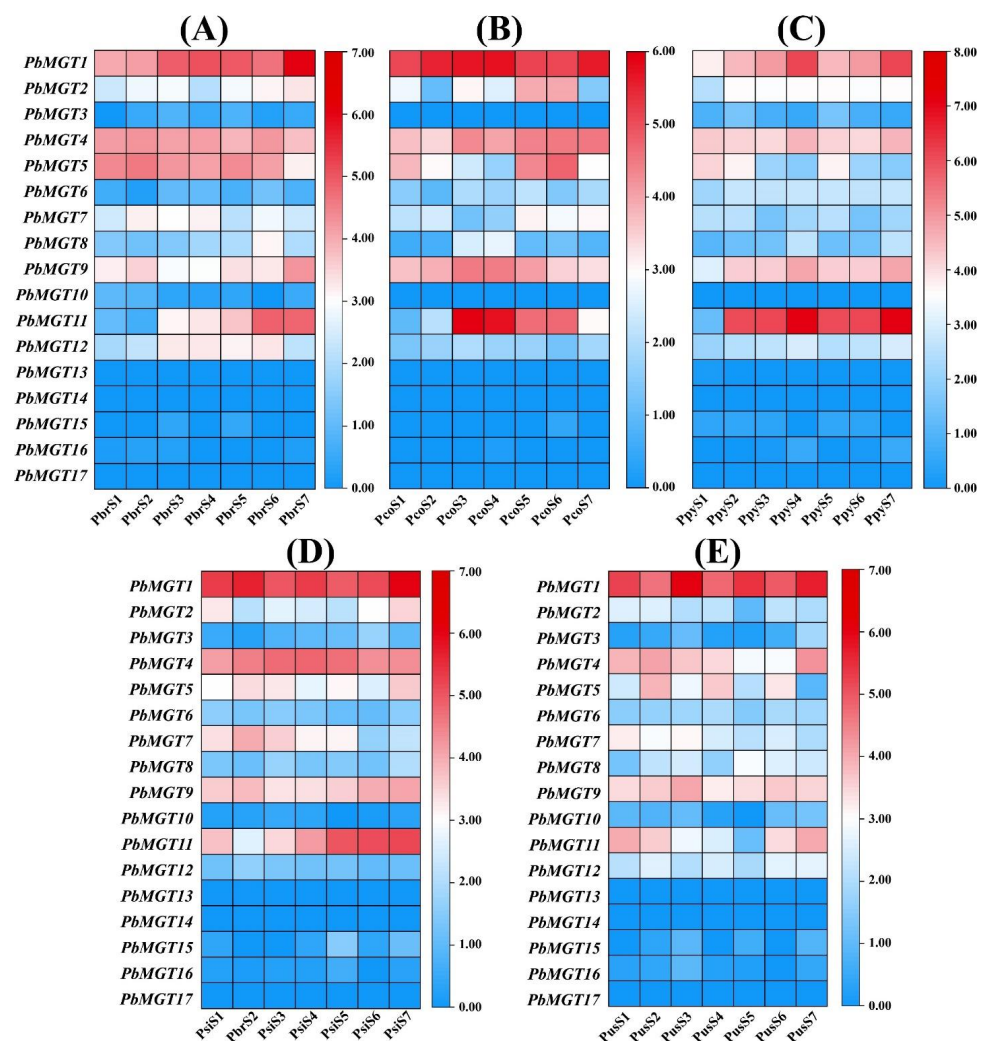


**Figure 13.** Transcript expression profiles of the *PbMGT* gene family visualized as a heat map using RNA-seq data, including (A) *Pyrus bretschneideri* (Pbr), (B) *Pyrus communis* (Pco), (C) *Pyrus pyrifolia* (Ppy), (D) *Pyrus sinkiangensis* (Psi), and (E) *Pyrus ussuriensis* (Pus). Seven developmental stages were collected, including fruit-setting period at 15 days after full blooming (15 DAB, period 1 [S1]), physiological fruit-dropping stage at 30 DAB (period 2 [S2]), fruit rapid enlargement stage at 55 DAB (period 3 [S3]), a month after fruit enlargement stage at 85 DAB (period 4 [S4]), premature stage at 115 DAB (period 5 [S5]), mature stage (duration varies by species, period 6 [S6]), and fruit senescence stage (period 7 [S7]). Ttools software generated the heatmap. The red boxes indicate increased gene expression, while the blue boxes represent decreased gene expression.

### 3.13. Graphical Representation of *PbMGT5* in Pear Tissues

Following its high expression in all five pear species, we draw a visual depiction of *PbMGT5* expression in pear tissues (Figure 14). As shown in the model (Figure 14), the *PbMGT5* gene showed significant expression levels throughout the pear life cycle. Given this, *PbMGT5* could be utilized as a marker to study its function in fruit development when exposed to magnesium stress.

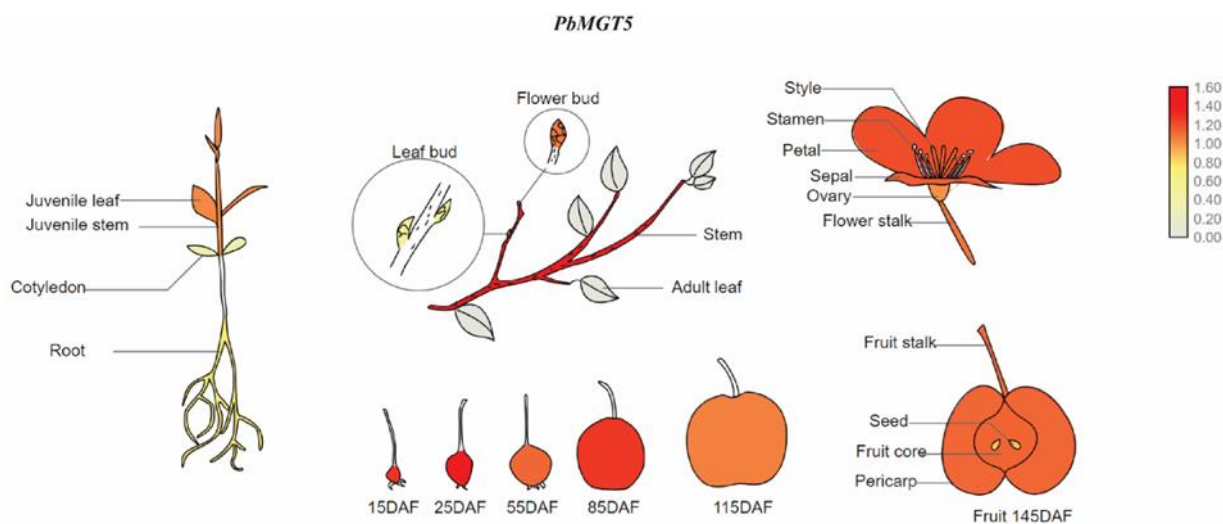


**Figure 14.** A schematic showing the distribution of *PbMGT5* expression in various Chinese white pear tissues. Various organs' names are shown. The white grey indicates modest expression, while the dark red indicates high expression.

## 4. Discussion

Magnesium (Mg) is involved in photosynthetic and metabolic processes and is a fundamental ingredient for plant growth and an essential cofactor [30,31]. A necessary role of magnesium transporters (MGTs) is the transfer and maintenance of magnesium concentrations in different cellular and organelle tissues [32]. Herein, we identified 17 *PbMGT* genes in the pear genome and conducted numerous bioinformatics and expression analyses.

### 4.1. *PbMGT* Are Widespread in Pears

The majority of the genes featured the conserved Mrs2\_Mfm1p-like motifs (Figure 1). According to [7], these motifs are crucial for MGTs' magnesium transport activities. Some plant species have more MGTs than others because of evolutionary processes, including duplication and polyploidization [5]. In addition, the investigated species showed nearly identical physicochemical traits and gene structures, lending credence to this theory. The NIPAs demonstrated a notable distinction from the other two subclasses of MGTs, which were MSR2 and CorA, respectively. For example, the NIPAs were anticipated to be stable proteins. Furthermore, the NIPAs were anticipated to be hydrophilic proteins using GRAVY as a solubility index [3]. Due to their distinct architectures, additional research into the functional analysis of NIPA classes in plants is required to fill the gaps in our understanding of their roles. In addition, the number of exons varied among *MGT* family members, particularly in the NIPAs, according to the gene structure study (Figure 5). Variation in the number of exons influences post-transcriptional processes like alternative splicing, which in turn increases the diversity of a gene's coding protein [4,7]. Genes that have fewer exons are better able to respond quickly to stress and thus are more important in the process of adjusting to harsh environmental conditions [33]. The *MGT* gene family members can be grouped into three primary categories based on phylogenetic study; orthologous NIPAs showed more diversity than CorA and MSR2. Compared to CorA and MSR2, the NIPAs' evolutionary mechanisms seemed unique (Figure 3).

Genomic analysis of *PbMGT* genes revealed an unequal distribution of these genes across the chromosomes of the pear genome (Figure 2). On specific chromosomes, however, the genes belonging to the various subfamilies are clustered unevenly. Genes belonging to the same subfamily could be located on different chromosomes, which indicates a distinct relationship between the structure and function of subfamilies [33].

#### 4.2. *PbMGT* Participates in a Wide Range of Biological Activities

Our findings show that the *PbMGT* gene family responds to abiotic stressors, binds ions, and transports metals. For example, in GO analysis, ion homeostasis (Figure 7) determines the outcome of the body's natural reaction to abiotic stresses and is directly impacted by most *PbMGT* genes [33,34]. This data points to the importance of *PbMGT* genes in regulating pear plant growth in controlled and stressed environments. Any molecular or biological process occurring within a plant cell relies on cis-acting elements [35–37]. Here, cis-elements associated with hormones, stress, and growth were found in the promoter region of the *PbMGT* genes (Figure 10). This category includes essential hormone-regulating elements ABRE, the TGA element, and stress-related elements like MYB, MYC, STRE, LTR, and MBS (Figure 10). This suggests that *PbMGT* genes are sensitive to stress and may provide a biomarker for creating plants that can withstand such conditions.

New developments in plant biotechnology have revealed a family of tiny regulatory RNA molecules known as microRNAs (miRNAs), which might be the key to unlocking these mysteries [27,38]. miRNAs are class of post-transcriptional gene regulators that play an important role in plant development and growth regulation by influencing the expression of specific genes [39]. Several members of *PbMGT* were cleaved to a series of miRNAs that furthered their involvement in key developmental processes. For instance, Our gene *PbMGT7* cleaved to miR169 and miR164, whereas *PbMGT1* cleaved to miR172, miR173, and miR414 (Figure 11). Enhanced adventitious root production in tobacco (*Nicotiana tabacum* L.) and apple (*Malus domestica*) was observed in the silenced *MdORE1* and overexpression of *mdm-miR164b* plants [40]. Evidence from genetic transformations in Arabidopsis lends credence to claims that grape *vvi-miR164b* is involved in many root development processes [41]. Reduced miR172 expression may be linked to enhanced Fe deficiency stress tolerance in citrus plants [42]. As a negative regulator of drought tolerance, miR169 and its targets (Nuclear TF Y subunit alpha, AtNFYA1, and NFYA5) decrease the expression of drought responsive genes [43]. Overall, the *MGT* gene family has been studied less in rosacea species and, therefore, needs extensive research to understand their functional role.

#### 4.3. Pear Reproductive Biology Alters by *PbMGT* Genes

The crop yield is determined by the anticipated progress of two crucial stages of reproductive biology, which include flower and fruit development. By interfering with metabolic and cellular processes, heavy metals can impact fruit and flower growth [33,44–46]. However, manipulating other factors like nutrients and hormones can reshape their involvement in the reproductive stages. The development of flowers and fruits is mainly regulated by hormones [47,48]. Furthermore, nutrients are critical for the plant's overall health, which controls its reproductive processes [49–51]. The high expression of various *PbMGT* genes during multiple phases of fruit development in distinct pear cultivars was the subject of our study (Figure 13). The *PbMGT1* had a high mRNA level at S1–S7. Substantial expression of *PbMGT4* and *PbMGT5* followed a comparable trend at S1–S7. The *PbMGT5* could be used as a marker to explore its role in pear subjected to magnesium stress. The soil toxicity puts a lot of pressure on fruit orchards. For instance, following exposure to aluminum, the expression levels of all *VvMGTs* genes exhibited an up-regulated pattern over time, with the exception of *VvMGT2*, which showed a reduction in expression. This implies that the reaction mechanism of the *VvMGT2* gene to aluminum may differ from that of other members [5]. This suggests that *MGT* genes may play a significant role in preserving the reproductive growth of plants in soil that has been damaged by heavy or light metals [52].

To prevent heavy metal damage throughout the flowering and fruit development stages, these biological molecules (*PbMGTs*) can be beneficial.

## 5. Conclusions

The pear genome database was searched, and 18 *PbMGT* genes were found. The phylogenetic study classified these genes into three distinct groups, namely NIPA, MERS2, and CorA. GO and *cis*-acting elements of *PbMGT* genes were involved in growth, reproduction, and stress biology. The results of the interacting protein study showed that *PbMGT* might control critical reproductive and developmental processes when paired with other proteins. The involvement of *PbMGT* in processes associated with growth was made apparent by their gene expression in various tissues. Their significance in controlling fruit developmental processes is further shown by the detailed expression of *PbMGT* genes in five pear cultivars. Although important *in silico* components and expression-based studies shed light on several features of *PbMGT*, their significance in fruit development should be further clarified by functional characterization of a couple of genes, *PbMGT5* in particular.

**Author Contributions:** Y.M. and B.D.: writing—original draft, data analysis, formal analysis. A.A.: data analysis, investigation. K.K.: writing—review and editing. Y.L.: data analysis, investigation. L.L.: writing—review and editing. Y.M., B.D. and L.L.: conceived and designed the experiments. All authors have read and agreed to the published version of the manuscript.

**Funding:** This research received no external funding.

**Data Availability Statement:** Data are contained within the article.

**Conflicts of Interest:** The authors declare no conflicts of interest.

## References

- Shahid, M.A.; Liu, G. Application of biostimulants to improve tomato yield in Florida. *Veg. Res.* **2022**, *2*, 6. [\[CrossRef\]](#)
- Heidari, P.; Abdullah; Faraji, S.; Poczai, P. Magnesium transporter Gene Family: Genome-Wide Identification and Characterization in *Theobroma cacao*, *Corchorus capsularis*, and *Gossypium hirsutum* of Family Malvaceae. *Agronomy* **2021**, *11*, 1651. [\[CrossRef\]](#)
- Bin, M.; Yi, G.; Zhang, X. Discovery and characterization of magnesium transporter (MGT) gene family in *Citrus sinensis* and their role in magnesium deficiency stress. *Plant Growth Regul.* **2023**, *100*, 733–746. [\[CrossRef\]](#)
- Wang, Y.; Hua, X.; Xu, J.; Chen, Z.; Fan, T.; Zeng, Z.; Wang, H.; Hour, A.-L.; Yu, Q.; Ming, R.; et al. Comparative genomics revealed the gene evolution and functional divergence of magnesium transporter families in *Saccharum*. *BMC Genom.* **2019**, *20*, 83. [\[CrossRef\]](#)
- Ge, M.; Zhong, R.; Sadeghnezhad, E.; Hakeem, A.; Xiao, X.; Wang, P.; Fang, J. Genome-wide identification and expression analysis of magnesium transporter gene family in grape (*Vitis vinifera*). *BMC Plant Biol.* **2022**, *22*, 217. [\[CrossRef\]](#)
- Mohamadi, S.F.; Babaeian Jelodar, N.; Bagheri, N.; Nematzadeh, G.; Hashemipetroudi, S.H. New insights into comprehensive analysis of magnesium transporter (MGT) gene family in rice (*Oryza sativa* L.). *3 Biotech* **2023**, *13*, 322. [\[CrossRef\]](#)
- Heidari, P.; Puresmaeli, F.; Mora-Poblete, F. Genome-Wide Identification and Molecular Evolution of the Magnesium Transporter (MGT) Gene Family in *Citrullus lanatus* and *Cucumis sativus*. *Agronomy* **2022**, *12*, 2253. [\[CrossRef\]](#)
- Gebert, M.; Meschenmoser, K.; Svidová, S.a.; Weghuber, J.; Schweyen, R.; Eifler, K.; Lenz, H.; Weyand, K.; Knoop, V. A Root-Expressed Magnesium Transporter of the *MRS2/MGT* Gene Family in *Arabidopsis thaliana* Allows for Growth in Low-Mg<sup>2+</sup> Environments. *Plant Cell* **2009**, *21*, 4018–4030. [\[CrossRef\]](#)
- Liu, G.; Yu, H.; Yuan, L.; Li, C.; Ye, J.; Chen, W.; Wang, Y.; Ge, P.; Zhang, J.; Ye, Z.; et al. *SIRCM1*, which encodes tomato Lutescent1, is required for chlorophyll synthesis and chloroplast development in fruits. *Hortic. Res.* **2021**, *8*, 128. [\[CrossRef\]](#)
- Sun, B.; Jiang, M.; Zheng, H.; Jian, Y.; Huang, W.-L.; Yuan, Q.; Zheng, A.-H.; Chen, Q.; Zhang, Y.-T.; Lin, Y.-X.; et al. Color-related chlorophyll and carotenoid concentrations of Chinese kale can be altered through CRISPR/Cas9 targeted editing of the carotenoid isomerase gene *BoaCRTISO*. *Hortic. Res.* **2020**, *7*, 161. [\[CrossRef\]](#)
- Chen, Z.C.; Yamaji, N.; Motoyama, R.; Nagamura, Y.; Ma, J.F. Up-Regulation of a Magnesium Transporter Gene *OsMGT1* Is Required for Conferring Aluminum Tolerance in Rice. *Plant Physiol.* **2012**, *159*, 1624–1633. [\[CrossRef\]](#)
- Chen, J.; Li, L.-G.; Liu, Z.-H.; Yuan, Y.-J.; Guo, L.-L.; Mao, D.-D.; Tian, L.-F.; Chen, L.-B.; Luan, S.; Li, D.-P. Magnesium transporter *AtMGT9* is essential for pollen development in *Arabidopsis*. *Cell Res.* **2009**, *19*, 887–898. [\[CrossRef\]](#)
- Chen, Z.C.; Yamaji, N.; Horie, T.; Che, J.; Li, J.; An, G.; Ma, J.F. A Magnesium Transporter *OsMGT1* Plays a Critical Role in Salt Tolerance in Rice. *Plant Physiol.* **2017**, *174*, 1837–1849. [\[CrossRef\]](#)
- Saquet, A.A.; Almeida, D. Sensory and instrumental assessments during ripening of ‘Rocha’ pear: The role of temperature and the inhibition of ethylene action on fruit quality. *Technol. Hortic.* **2023**, *3*, 23. [\[CrossRef\]](#)

15. Zhang, H.; Han, W.; Linghu, T.; Zhao, Z.; Wang, A.; Zhai, R.; Yang, C.; Xu, L.; Wang, Z. Overexpression of a pear B-class MAD5-box gene in tomato causes male sterility. *Fruit. Res.* **2023**, *3*, 1. [\[CrossRef\]](#)
16. Zhang, H.; Liu, X.; Tang, C.; Lv, S.; Zhang, S.; Wu, J.; Wang, P. PbrbohH/J mediates ROS generation to regulate the growth of pollen tube in pear. *Plant Physiol. Biochem.* **2024**, *207*, 108342. [\[CrossRef\]](#)
17. Li, X.; Qi, L.; Zang, N.; Zhao, L.; Sun, Y.; Huang, X.; Wang, H.; Yin, Z.; Wang, A. Integrated metabolome and transcriptome analysis of the regulatory network of volatile ester formation during fruit ripening in pear. *Plant Physiol. Biochem.* **2022**, *185*, 80–90. [\[CrossRef\]](#)
18. Zhang, M.-Y.; Xue, C.; Xu, L.; Sun, H.; Qin, M.-F.; Zhang, S.; Wu, J. Distinct transcriptome profiles reveal gene expression patterns during fruit development and maturation in five main cultivated species of pear (*Pyrus L.*). *Sci. Rep.* **2016**, *6*, 28130. [\[CrossRef\]](#)
19. Ahmad, S.; Jeridi, M.; Siddiqui, S.; Ali, S.; Shah, A.Z. Genome-wide identification, characterization, and expression analysis of the Chalcone Synthase gene family in *Oryza sativa* under Abiotic Stresses. *Plant Stress.* **2023**, *9*, 100201. [\[CrossRef\]](#)
20. Chen, C.; Chen, H.; He, Y.; Xia, R. TBtools, a toolkit for biologists integrating various biological data handling tools with a user-friendly interface. *BioRxiv* **2018**, 289660.
21. Ahmad, S.; Ali, S.; Shah, A.Z.; Khan, A.; Faria, S. Chalcone synthase (CHS) family genes regulate the growth and response of cucumber (*Cucumis sativus L.*) to *Botrytis cinerea* and abiotic stresses. *Plant Stress.* **2023**, *8*, 100159. [\[CrossRef\]](#)
22. Tan, Y.; Xiao, L.; Zhao, J.; Zhang, J.; Ahmad, S.; Xu, D.; Xu, G.; Ge, L. Adenosine Monophosphate-Activated Protein Kinase (AMPK) Phosphorylation Is Required for 20-Hydroxyecdysone Regulates Ecdysis in *Apolygus lucorum*. *Int. J. Mol. Sci.* **2023**, *24*, 8587. [\[CrossRef\]](#)
23. Ahmad, S.; Chen, Y.; Shah, A.Z.; Wang, H.; Xi, C.; Zhu, H.; Ge, L. The Homeodomain-Leucine Zipper Genes Family Regulates the Jinglyngmycin Mediated Immune Response of *Oryza sativa* to *Nilaparvata lugens*, and *Laodelphax striatellus*. *Bioengineering* **2022**, *9*, 398. [\[CrossRef\]](#)
24. Ullah, U.; Shalmani, A.; Ilyas, M.; Raza, A.; Ahmad, S.; Shah, A.Z.; Khan, F.U.; AzizUd, D.; Bibi, A.; Rehman, S.U.; et al. BZR proteins: Identification, evolutionary and expression analysis under various exogenous growth regulators in plants. *Mol. Biol. Rep.* **2022**, *49*, 12039–12053. [\[CrossRef\]](#)
25. Ahmad, S.; Zhu, H.; Chen, Y.; Xi, C.; Shah, A.Z.; Ge, L. Comprehensive Bioinformatics and Expression Analysis of the TLP Gene Family Revealed Its Role in Regulating the Response of *Oryza sativa* to *Nilaparvata lugens*, *Laodelphax striatellus*, and Jinglyngmycin. *Agronomy* **2022**, *12*, 1297. [\[CrossRef\]](#)
26. Lescot, M.; Déhais, P.; Thijs, G.; Marchal, K.; Moreau, Y.; Van de Peer, Y.; Rouzé, P.; Rombauts, S. PlantCARE, a database of plant cis-acting regulatory elements and a portal to tools for in silico analysis of promoter sequences. *Nucleic Acids Res.* **2002**, *30*, 325–327. [\[CrossRef\]](#)
27. Raza, A.; Charagh, S.; Karikari, B.; Sharif, R.; Yadav, V.; Mubarak, M.S.; Habib, M.; Zhuang, Y.; Zhang, C.; Chen, H.; et al. miRNAs for crop improvement. *Plant Physiol. Biochem.* **2023**, *201*, 107857. [\[CrossRef\]](#)
28. Kelley, L.A.; Mezulis, S.; Yates, C.M.; Wass, M.N.; Sternberg, M.J.E. The Phyre2 web portal for protein modeling, prediction and analysis. *Nat. Protoc.* **2015**, *10*, 845–858. [\[CrossRef\]](#)
29. Li, F.; Zhang, L.; Ji, H.; Xu, Z.; Zhou, Y.; Yang, S. The specific W-boxes of GAPC5 promoter bound by TaWRKY are involved in drought stress response in wheat. *Plant Sci. Int. J. Exp. Plant Biol.* **2020**, *296*, 110460. [\[CrossRef\]](#)
30. Ishfaq, M.; Wang, Y.; Yan, M.; Wang, Z.; Wu, L.; Li, C.; Li, X. Physiological Essence of Magnesium in Plants and Its Widespread Deficiency in the Farming System of China. *Front. Plant Sci.* **2022**, *13*, 802274. [\[CrossRef\]](#)
31. Tränkner, M.; Tavakol, E.; Jáklí, B. Functioning of potassium and magnesium in photosynthesis, photosynthate translocation and photoprotection. *Physiol. Plant.* **2018**, *163*, 414–431. [\[CrossRef\]](#)
32. Tian, X.-Y.; He, D.-D.; Bai, S.; Zeng, W.-Z.; Wang, Z.; Wang, M.; Wu, L.-Q.; Chen, Z.-C. Physiological and molecular advances in magnesium nutrition of plants. *Plant Soil.* **2021**, *468*, 1–17. [\[CrossRef\]](#)
33. Xu, R.; Ali, A.; Li, Y.; Zhang, X.; Sharif, R.; Feng, X.; Ding, B. Transcriptome-Wide Analysis Revealed the Influential Role of PbrMTP (Metal Tolerance Protein) in the Growth and Fruit Development of Chinese White Pear. *J. Plant Growth Regul.* **2023**. [\[CrossRef\]](#)
34. Shalmani, A.; Ullah, U.; Muhammad, I.; Zhang, D.; Sharif, R.; Jia, P.; Saleem, N.; Gul, N.; Rakhmanova, A.; Tahir, M.M.; et al. The TAZ domain-containing proteins play important role in the heavy metals stress biology in plants. *Environ. Res.* **2021**, *197*, 111030. [\[CrossRef\]](#)
35. Pan, J.; Tu, J.; Sharif, R.; Qi, X.; Xu, X.; Chen, X. Study of JASMONATE ZIM-Domain gene family to waterlogging stress in *Cucumis sativus L.* *Veg. Res.* **2021**, *1*, 3. [\[CrossRef\]](#)
36. Sharif, R.; Xie, C.; Wang, J.; Cao, Z.; Zhang, H.; Chen, P.; Yuhong, L. Genome wide identification, characterization and expression analysis of HD-ZIP gene family in *Cucumis sativus L.* under biotic and various abiotic stresses. *Int. J. Biol. Macromol.* **2020**, *158*, 502–520. [\[CrossRef\]](#)
37. Jia, P.; Sharif, R.; Li, Y.; Sun, T.; Li, S.; Zhang, X.; Dong, Q.; Luan, H.; Guo, S.; Ren, X.; et al. The BELL1-like homeobox gene MdBLH14 from apple controls flowering and plant height via repression of MdGA20ox3. *Int. J. Biol. Macromol.* **2023**, *242*, 124790. [\[CrossRef\]](#)
38. Sharif, R.; Raza, A.; Chen, P.; Li, Y.; El-Ballat, E.M.; Rauf, A.; Hano, C.; El-Esawi, M.A. HD-ZIP Gene Family: Potential Roles in Improving Plant Growth and Regulating Stress-Responsive Mechanisms in Plants. *Genes* **2021**, *12*, 1256. [\[CrossRef\]](#)

39. Wang, Y.; Luo, Z.; Zhao, X.; Cao, H.; Wang, L.; Liu, S.; Wang, C.; Liu, M.; Wang, L.; Liu, Z. Superstar microRNA, miR156, involved in plant biological processes and stress response: A review. *Sci. Hortic.* **2023**, *316*, 112010. [[CrossRef](#)]
40. Fan, X.; Li, H.; Guo, Y.; Sun, H.; Wang, S.; Qi, Q.; Jiang, X.; Wang, Y.; Xu, X.; Qiu, C.; et al. Integrated multi-omics analysis uncovers roles of mdm-miR164b-MdORE1 in strigolactone-mediated inhibition of adventitious root formation in apple. *Plant Cell Env.* **2022**, *45*, 3582–3603. [[CrossRef](#)]
41. Zhang, L.; Chen, Q.; Liu, J.; Dou, F.; Wang, H.; Song, Y.; Ren, Y.; He, J.; Wang, L.; Zhang, C.; et al. Identification of grape miRNA revealed Vvi-miR164b involved in auxin induced root development. *Sci. Hortic.* **2022**, *295*, 110804. [[CrossRef](#)]
42. Jin, L.F.; Yarra, R.; Yin, X.X.; Liu, Y.Z.; Cao, H.X. Identification and function prediction of iron-deficiency-responsive microRNAs in citrus leaves. *3 Biotech* **2021**, *11*, 121. [[CrossRef](#)]
43. Sorin, C.; Declerck, M.; Christ, A.; Blein, T.; Ma, L.; Lelandais-Brière, C.; Njo, M.F.; Beeckman, T.; Crespi, M.; Hartmann, C. A miR169 isoform regulates specific NF-YA targets and root architecture in Arabidopsis. *New Phytol.* **2014**, *202*, 1197–1211. [[CrossRef](#)]
44. Sharif, R.; Su, L.; Chen, X.; Qi, X. Involvement of auxin in growth and stress response of cucumber. *Veg. Res.* **2022**, *2*, 13. [[CrossRef](#)]
45. Sharif, R.; Su, L.; Chen, X.; Qi, X. Hormonal interactions underlying parthenocarpic fruit formation in horticultural crops. *Hortic. Res.* **2022**, *9*, uhab024. [[CrossRef](#)]
46. Su, L.; Rahat, S.; Ren, N.; Kojima, M.; Takebayashi, Y.; Sakakibara, H.; Wang, M.; Chen, X.; Qi, X. Cytokinin and auxin modulate cucumber parthenocarpic fruit development. *Sci. Hortic.* **2021**, *282*, 110026. [[CrossRef](#)]
47. Su, L.; Wang, M.; Wang, Y.; Sharif, R.; Ren, N.; Qian, C.; Xu, J.; Chen, X.; Qi, X. Forchlorfenuron Application Induced Parthenocarpic Fruit Formation without Affecting Fruit Quality of Cucumber. *Horticulturae* **2021**, *7*, 128. [[CrossRef](#)]
48. Jia, P.; Wang, Y.; Sharif, R.; Ren, X.; Qi, G. *MdIPT1*, an adenylate isopentenyltransferase coding gene from *Malus domestica*, is involved in branching and flowering regulation. *Plant Sci.* **2023**, *333*, 111730. [[CrossRef](#)]
49. Prasad, R. Cytokinin and Its Key Role to Enrich the Plant Nutrients and Growth Under Adverse Conditions-An Update. *Front. Genet.* **2022**, *13*, 883924. [[CrossRef](#)]
50. Ahmed, N.; Zhang, B.; Bozdar, B.; Chachar, S.; Rai, M.; Li, J.; Li, Y.; Hayat, F.; Chachar, Z.; Tu, P. The power of magnesium: Unlocking the potential for increased yield, quality, and stress tolerance of horticultural crops. *Front. Plant Sci.* **2023**, *14*, 1285512. [[CrossRef](#)]
51. Jiao, J.; Li, J.; Chang, J.; Li, J.; Chen, X.; Li, Z.; Song, Z.; Xie, D.; Zhang, B. Magnesium Effects on Carbohydrate Characters in Leaves, Phloem Sap and Mesocarp in Wax Gourd (*Benincasa hispida* (Thunb.) Cogn.). *Agronomy* **2023**, *13*, 455. [[CrossRef](#)]
52. Hou, D.; O'Connor, D.; Igalavithana, A.D.; Alessi, D.S.; Luo, J.; Tsang, D.C.W.; Sparks, D.L.; Yamauchi, Y.; Rinklebe, J.; Ok, Y.S. Metal contamination and bioremediation of agricultural soils for food safety and sustainability. *Nat. Rev. Earth Environ.* **2020**, *1*, 366–381. [[CrossRef](#)]

**Disclaimer/Publisher's Note:** The statements, opinions and data contained in all publications are solely those of the individual author(s) and contributor(s) and not of MDPI and/or the editor(s). MDPI and/or the editor(s) disclaim responsibility for any injury to people or property resulting from any ideas, methods, instructions or products referred to in the content.